Influence of the substrate's surface morphology and chemical nature on the nucleation and growth of microcrystalline silicon.

E. Vallat-Sauvain, J. Bailat, J. Meier, X. Niquille, U. Kroll and A. Shah

Institut de Microtechnique, Université de Neuchâtel, Breguet 2, CH-2000 Neuchâtel, Switzerland

Phone +41 32 718 32 00, fax +41 32 718 32 01

e-mail: Evelyne.Vallat@unine.ch

Abstract

Hydrogenated microcrystalline silicon (μc-Si:H) layers about 500 nm thick were deposited in the same run on flat and rough substrates (rms = 60 nm) of various chemical nature. This study reveals that the spatial distribution of the microcrystalline/amorphous phases within the layer depends on the substrate's topography. The influence of the chemical nature of the substrate is shown to be preponderant on the layers nucleation. In particular, this study shows that nucleation density is the highest on plasma enhanced chemical vapor deposited silicon dioxide, whereas it is independent of the substrate's surface topography. Finally, the interpretation of Micro-Raman experiments for the evaluation of the respective volume fractions of amorphous/microcrystalline phases in the layers is discussed in relation with their spatial distribution.

Keywords: Nucleation (327), Silicon (434), Raman Scattering (403), Transmission Electron Microscopy (496)

Section A (Synthesis and characterization)

1.Introduction

Hydrogenated microcrystalline silicon (µc-Si:H) is a material of choice for large-area thin film electronics such as photovoltaics and thin-film transistors. This material exhibits a complex microsctructure composed of the microcrystalline phase (nanocrystals+grain boundaries) and amorphous silicon [1-3]. It is well known that the substrate chemical nature and crystallinity on which microcrystalline silicon growth takes place plays a critical role on the resulting layers microstructure [4]. In particular, substrate topography has been shown to be determinant for growth direction of the microcrystalline material, as it starts perpendicular to the local substrate plane [5,6]. Thus, when growth takes place on steep structures, columnar growth of microcrystalline grains collides over substrate grooves, producing, thus, grain boundaries that extend from the bottom right up to the top of the layers [6]. Furthermore, due to this growth process, amorphous silicon is found preferentially at the bottom of substrate grooves. The density of microcrystalline silicon nuclei on various substrates has been shown to depend on the chemical nature of the substrate [7]. It was shown that silicon nitride inhibits nucleation, whereas silicon dioxyde promotes it.

Studies on the role of the chemical nature of the susbtrates on nucleation have been conducted only on flat substrates, whereas study on the effect of substrate's roughness on growth were conducted only on substrates of identical chemical nature. Thus, it is the aim of this paper to the study the combined effect of both the chemical and crystallographic nature and the topography of the substrate on microcrystalline silicon nucleation and growth. The susbtrate roughness chosen here has a rms value of approx. 60 nm, typically used for improved light trapping in photovoltaic applications. The results of our observations do not show intricate effects of chemical nature and topography of substrate on nucleation and growth ; they can be simply summerized as follows : a) the nucleation density depends on the chemical nature of the substrate and not on its topography, b)substrate topography has a manifest influence on

the spatial distribution of the amorphous and microcrystalline phases. This leads to depth-sensitive Raman crystallinity values.

These observations are of importance for a better mastering of the nucleation and growth of μc-Si:H layers, in particular for photovoltaic applications, where the crystallinity of the material and its spatial distribution within the cell have been shown to be of critical importance with respect to the electrical characteristics of the device [8].

2. Experimental details

Microcrystalline silicon layers were deposited on different substrates in the same run. The deposition conditions were plasma excitation frequency of 110 MHz, a substrate temperature of 180 ^{o}C, a chamber pressure of 0.3 mbar and silane/hydrogen gas phase concentration of 5 %, yielding microcrystalline material close to the amorphous/microcrystalline transition. Rough substrates with a similar surface topography (rms 55-60 nm), but of different chemical nature were obtained by covering conformally low pressure chemical vapor deposited (LPCVD) zinc oxyde (ZnO) transparent conducting oxide coated glass substrates with a very thin (less than 20 nm) layer of a specific materials, with different chemical and structural nature. The surface topography of LPCVD-ZnO typically consists of random pyramids with an average basis of a few hundreds nm and a rms roughness of 55-60 nm [9]. This rough substrate will be noted R-ZnO (where R stands for rough). Surfaces having a statistically defined and identical topography but consisting of rough sputtered ZnO (R-sZnO), rough plasma enhanced chemical vapor deposited (PECVD) SiO2 (denoted here R-SiO_2) and rough chromium (R-Cr) were obtained in addition to the initial R-ZnO. A μc-Si:H layer was then deposited on the resulting substrates. For purposes of comparison, μc-Si:H layers were also deposited on flat sputtered ZnO (F-sZnO) and flat PECVD SiO_2 (F-SiO2) coated glass, as well as on standard cleaned glass (AF45). The microcrystalline silicon layer was deposited on the seven substrates (of size 4 cm x 4 cm) in the same run. Due to the different roughness of the substrates used here, the thickness of the microcrystalline silicon layer (measured

perpendicularily to the average substrate plane) varied from 550 nm on the flat substrates down to 350 nm on the rough substrate. This difference in thickness for layers co-deposited in the same run is typical of deposition in the depletion regime where growth is limited by the flux of adatoms on the substrate surface [10]. In our case, the effective area of rough substrates is larger than that on flat substrate. The layer thickness on the latter is thus larger. The layer crystallinity was characterized by Micro-Raman spectroscopy in the backscattering configuration with the 633 nm excitation line of a HeNe laser, with the light impinging on the top of the microcrystalline layer. The Raman signal (proportional to the excited volume) decreases exponentially with depth because of the laser beam absorption within the material. This effect defines the depth-sensitivity of the Raman measurement technique. For the excitation used here (HeNe laser at 633 nm), the absorption coefficient in μc-Si:H is about 1 μm and consequently, the Raman collection depth is 0.5 μm, approximatively equivalent to the sample thickness [11]. The Raman signal was deconvoluted into three peaks, whose integrated scattered intensities were evaluated assuming Gaussian shapes. The narrow line at 520 cm^{-1} and its tail at 510 cm^{-1} are attributed to the microcrystalline phase of the material and their scattered intensities $I_{520}+I_{510}= I_c$, whereas the broad peak at about 480 cm^{-1} is attributed to the amorphous phase of the material. Its integrated intensity yields I_a. The Raman crystallinity factor (ϕ_c), which is the highest bound of the layer's crystallinity [11], is defined as $\phi_c = I_c/(I_c+I_a)$. The layer microstructure was investigated with transmission electron microscopy (TEM). Layer cross-sections were prepared by mechanical polishing and then observed in a Philips CM200 microscope operated at 200 kV. The average layer crystallinity ϕ_{cTEM} was evaluated by micrograph digitalization (the microcrystalline phase being drawn black on a transparent, then digitalized and the ratio of black/white surface evaluated numerically). Note here that microcrystalline material is made of nanocrystals and amorphous grain boundaries, the fraction of which cannot be evaluated on our TEM micrographs due the medium resolution used in the imaging conditions. Thus ϕ_{cTEM} values up to 95 % were

measured in the highly crystalline layers. On the other hand, Micro-Raman is sensitive to the presence of the amorphous material (grain boundaries) within microcrystalline silicon and largest ϕ_c values are slightly above 80 % in highly microcrystalline material. The nuclei density was measured by hand on the TEM micrographs, as the number of silicon nanocrystals per linear, (rough) substrate's unit length (see Fig.2).

3. Results

Fig.1. shows the microstructure of the microcrystalline silicon layers deposited in the same run on rough substrates. As expected, the substrates's surface roughness are comparable and conical conglomerates of nano-crystals (i.e. the microcrystalline phase) separated by amorphous phase and/or voids can be observed on each of the three micrographs. A closer look, however, shows that the crystalline fraction and the nuclei density increases from micrograph a) to c), as shown in Fig.3 . The microcrystalline phase nucleates directly on top of the substrate's pyramids, and the amorphous material is found at the bottom of the substrate's grooves, extending right up to the top of the layers, as sketeched in Fig.2. Fig.4 shows the Raman crystallinity factor ϕ_c measured from the top of the layers. One can note that on the rough substrates, ϕ_c increases steadily from 21 % to 32 % depending on the chemical nature of the substrate (note that in this sense LPCVD ZnO and sputtered ZnO are diffrent as they do not contain the same dopant : 3 % weight aluminium in sputtered ZnO and boron in the same order of magnitude in LPCVD ZnO ; furthermore LPCVD-ZnO and sputtered ZnO do not have the same crystallographic properties [9]). In this study, the lowest value of ϕ_c is measured for (flat and rough) sputtered ZnO, whereas the highest value for ϕ_c is observed for layers grown on PECVD-SiO_2. The TEM evaluation of the nuclei density (n_d) are given in Fig.3 as a function of the substrate type. For the two flat substrates (F-sZnO and F-SiO_2), TEM analysis shows that nuclei density is very different: 5 and 13 μm^{-1}, respectively. Surprisingly, the crystalline fraction estimated by Raman is very similar, approximatively 50 % for both samples. The explanation is given by the TEM micrographs (not shown here): the

amorphous material in both samples deposited on flat substrates is mainly lying at the bottom of the layer and does not reach the layer's top surface. This is opposite to what is observed for the layers grown on the rough substrates, where the amorphous material reaches the top of the layer. As the excitation beam (collection depth of 500 nm) of the Raman spectrometer enters the layer (550 nm thick) from its strongly microcrystalline top, it does not probe the amorphous phase lying at the bottom of the layer (early stages of growth). This effect is further enhanced by the difference of thickness between the layers grown on flat susbtrates (thickness 550 nm) and on rough susbtrates (thickness 350 nm).

One can note on Fig.3.b that the nuclei density is identical on flat and rough sputtered ZnO as well as on flat and rough PECVD silicon dioxide. This is an indication that nucleation of μc-Si:H does not depend on the substrate roughness, at least within the framework of the present study. On the other hand, on the rough susbtrates whenever n_d increases, ϕ_c increases as well (see Fig.5). For a given substrate roughness, a linear relationship between n_d and ϕ_c is observed.

4. Discussion

The independence of the nuclei density on the substrate's morphology is shown in Fig. 3.b. Hasegawa et al. [12] had already observed a similar behavior, but for much smaller substrate roughness (in the range of a few nm), not representative of typical substrate roughness used for efficient light trapping schemes within photovoltaic devices. Here, the preponderant role of the chemical nature of the substrate for μc-SiH nucleation is confirmed and shown to be valid also for substrates with higher roughness as typically used for efficient light trapping in μc-Si:H.

An unexpected result of this study is the observation of the largest nuclei density on PECVD-SiO_2. Indeed, earlier studies revealed that nucleation of μc-Si:H on glass is harder to obtain than on ZnO [13]. Consequently, surface chemistry of glass cannot be assumed to be similar to PECVD-SiO_2 , at least as far as nucleation of μc-Si:H is concerned. This has been observed

in our series of substrates where we remark that the Raman crystallinity factor of the layer grown on AF45 glass is 10 % (relative) lower compared to that on PECVD-SiO_2. One can, thus, expect that plasma pre-treated substrates may have varying nucleation densities compared with untreated substrates. Such an effect had been observed by Hu et al [14], who showed that the grain size of poly silicon deposited on glass or SiO_x depend on the presence of H.

The Micro-Raman measurements performed on layers deposited on flat substrates reveal the depth sensitivity of this technique. In the backscattering Raman configuration used here, the optical path consists of the transmitted plus backscattered path. Thus the absorption coefficient has to be doubled in the exponential attenuation factor of the excitation beam. One can calculate that a 50 nm continuous amorphous layer lying at the bottom of a 550 nm thick sample contributes only 6 % (instead of 9 % if proportional) to the Raman light collected on the sample surface [11]. Such continuous amorphous layers have been observed here by TEM in μcSi:H layers grown on the flat substrates. The amorphous fraction lying at the bottom of the layers are therefore under evaluated by Raman spectroscopy with the excitation beam entering the layer from the top. On the other hand, on the rough substrates, the amorphous fraction extends much higher in the layer and contributes, thus, proportionally more to the collected Raman signal. This is due to the effect of substrate roughness on μc-Si:H microstructure. Indeed, μc-Si:H starts growing perpendicular to the local substrate plane. On rough substrates, as studied here, the geometrical consequences of this growth process are an increased amorphous fraction in the substrates grooves, increasing, thus, the amorphous fraction at the bottom of the sample. The crystallinity at the bottom of the sample can be evaluated with Raman measurements performed with excitation light impinging on the first grown part (bottom) of the sample. Such measurements on flat substrates yield a bottom crystallinity that is about 20 % (relative) lower than the top crystallinity. Therefore, the

average crystalline fraction of the layer as measured from the TEM micrographs is a more reliable measurement technique of the layer cristallinity than Raman measurements.

5. Conclusions

It is well known from previous work that nucleation and growth depend on the chemical nature of flat substrates [4] ; on the other hand, spatial distribution of the amorphous and microcrystalline phases within a microcrystalline layer depend on the roughness of the substrates [6]. Until now, a study of the combined effect of both the chemical nature and substrate roughness on nucleation and growth of microcrystalline silicon layer was missing. Our observations show that both effects are independent, and can simply summerized as follows :

a) For both rough and flat substrates as studied here, the influence of the chemical nature of the substrate is shown to be preponderant on the layers nucleation. In particular, this study shows that nucleation density is the highest on PECVD-silicon dioxide, compared with Cr, sputtered ZnO and LPCVD ZnO.
b) The microcrystalline/amorphous phase spatial distribution within a microcrystalline silicon (μc-Si :H) layer depends on the substrate's topography.

Because growth of microcrystalline silicon locally starts perpendicular to the substrate facets, the Raman crystallinity factor measured on substrates with the same roughness increases with the nuclei density measured by TEM. However, Raman crystallinity factor measurements on layers deposited on flat substrates is independent of the nuclei density. This shows the sensitivity limits of this measurement technique: the crystallinity measured in this manner is overestimated as the amorphous material is lying mostly at the bottom of the layer.

Acknowledgements

This work was supported by the Swiss National Science Foundation under grant FN66985, as well as by the Swiss Federal Office of Energy (OFEN) under contract No. 36487.

References

[1] E. Vallat-Sauvain, U. Kroll, J. Meier, A. Shah, and J. Pohl, J. Appl. Phys. 87 (2000) 3137.
[2] M. Luysberg, C. Scholten, L. Houben, R. Carius, F. Finger, and O. Vetterl, Mat. Res. Soc. Symp. Proc. 664 (2001) A15.2.1.
[3] O. Vetterl, F. Finger, R. Carius, P. Hapke, L. Houben, O. Kluth, A. Lambertz, A. Muck, B. Rech, and H. Wagner, Solar Energy Materials and Solar Cells 62 (2000) 97.
[4] R. W. Collins, A. S. Ferlauto, G. M. Ferreira, C. Chen, Joohyun Koh, R. J. Koval, Yeeheng Lee, J. M. Pearce, and C. R. Wronski, Solar Energy Materials and Solar Cells 78 (2003) 143.
[5] J. Dubail, E. Vallat-Sauvain, J. Meier, S. Dubail, and A. Shah, Mat. Res. Soc. Symp. Proc. 609 (2001) A13.6.1.
[6] Y. Nasuno, M. Kondo, and A. Matsuda, Mat. Res. Soc. Symp. Proc. 664 (2001) A.15.5.1.
[7] J. Koh, A. S. Ferlauto, P. I. Rovira, C. R. Wronski, and R. W. Collins, Appl. Phys. Lett. 75 (1999) 2286.
[8] J. Bailat, E. Vallat-Sauvain, L. Feitknecht, C. Droz, and A. Shah, J. Appl. Phys. 93 (2003) 5727.
[9] S. Faÿ, U. Kroll, C. Bucher, E. Vallat-Sauvain, and A. Shah, to be published in Solar Energy Materials and Solar cells (2004).
[10] M. Heintze and R. Zedlitz, J. Non-Cryst. Sol. 198-200 (1993) 1038.
[11] C. Droz, E. Vallat-Sauvain, J. Bailat, L. Feitknecht, J. Meier, and A. Shah, Solar Energy Materials and Solar Cells 81 (2004) 61.
[12] S. Hasegawa, N. Uchida, S. Takenaka, T. Inokuma, and Y. Kurata, Jpn. J. Appl. Phys. 37 (1998) 4711.
[13] J. Bailat, E. Vallat-Sauvain, L. Feitknecht, C. Droz, and A. Shah, J. Non-Cryst. Sol. 299-302 (2002) 1219.
[14] Y. Z. Hu, C. Y. Zao, C. Basa, W. X. Gao, and E. A. Irene, Appl. Phys. Lett. 69 (1996) 485.

Figure captions

Fig.1: TEM bright field micrographs of μc-Si:H grown on a) i-layer on R-sZnO, b) i-layer on R-ZnO, c) i-layer on R-SiO_2.

Fig.2 : Schematic representation of μc-Si :H layer microstructure as observed in Fig.1. Nuclei are indicated by a small dot and the measured nuclei density n_d is shown. The microcrystalline phase consists of cones growing prependicular to the local substrate plane, colliding after the so-called coalescence threshold. Below the colaescence threshold, the material inbetween the cones is amorphous (grey on this sketch).

Fig.3: a) Crystalline fraction ϕ_{cTEM} and b) Nuclei density n_d (error on n_d is approximatively ±10%) evaluated from TEM sample section's micrographs, as a function of the substrate type. For both flat and rough substrates, PECVD silicon dioxyde is the most favourable layer for nucleation, whereas sputtered ZnO is the less favourable for nucleation.

Fig.4: Raman crystallinity factor ϕ_c as a function of the substrate type (error on $\phi_c$is ± 5%). R- stands for rough, whereas F- stands for flat.

Fig.5: Raman crystallinity factor ϕ_c as a function of the linear nuclei density of the rough substrates. The dotted line is the linear least square fit to the datas.

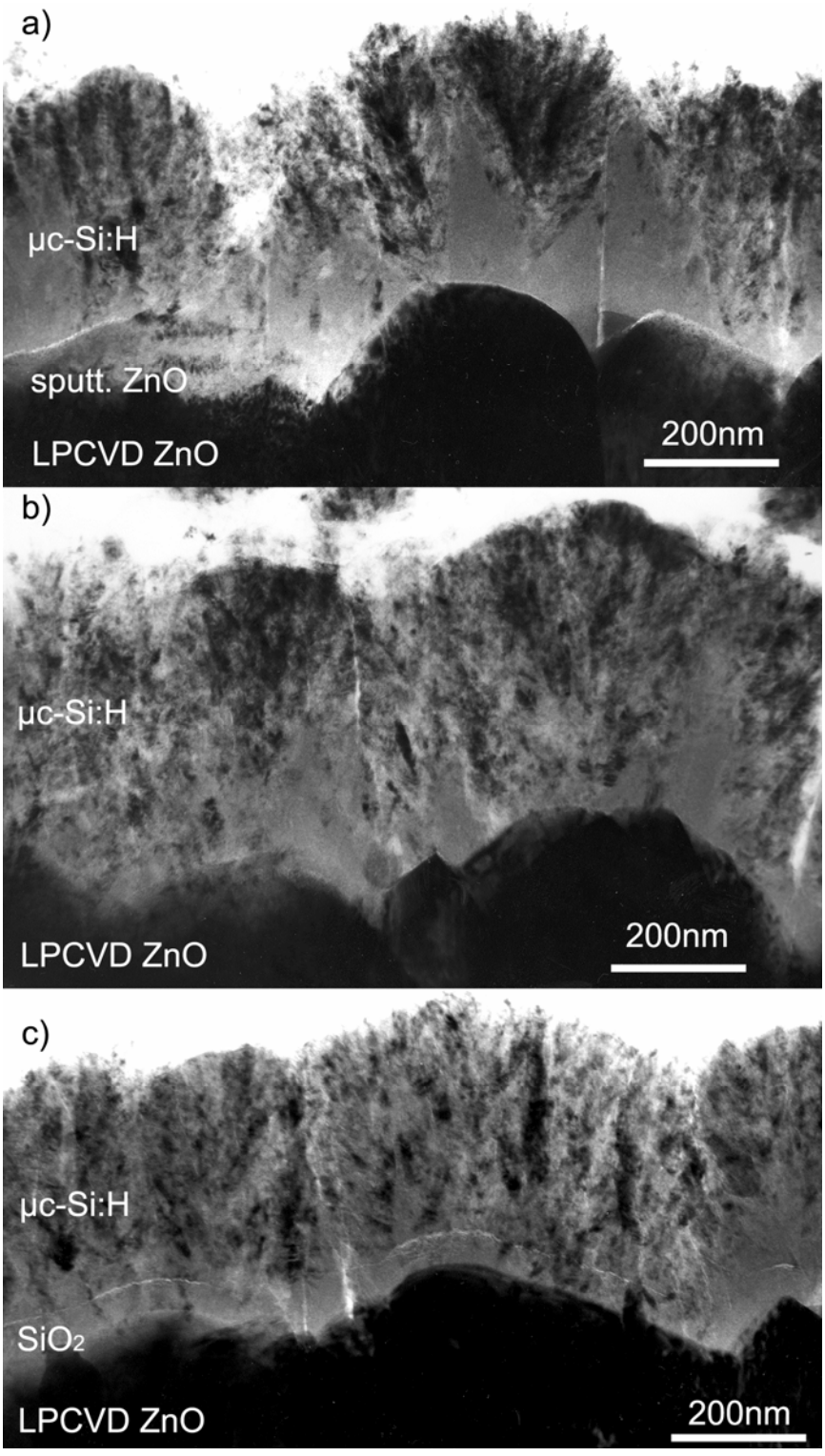
a)
µc-Si:H
sputt. ZnO
LPCVD ZnO
200nm
b)
µc-Si:H
LPCVD ZnO
200nm
c)
µc-Si:H
SiO2
LPCVD ZnO
200nm

Fig.1

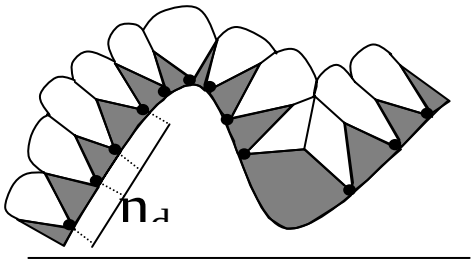

Fig.2

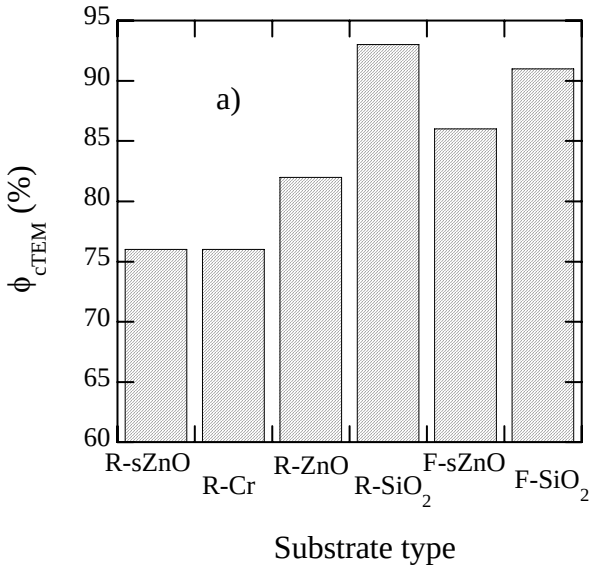
95
90
85
80
75
70
65
60
a)
ϕ_{cTEM} (%)
R-sZnO
R-Cr
R-ZnO
R-SiO2
F-sZnO
F-SiO2
Substrate type

Fig. 3.a

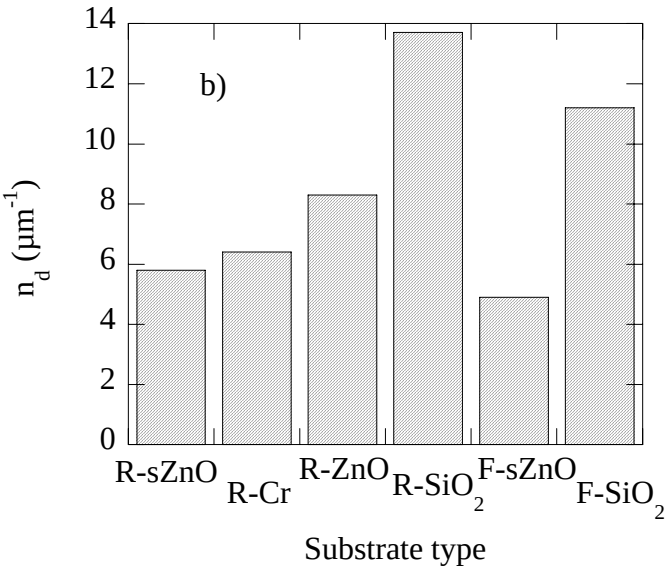
14
12
10
8
6
4
2
0
b)
n_d (μm^{-1})
R-sZnO
R-Cr
R-ZnO
R-SiO2
F-sZnO
F-SiO2
Substrate type

Fig. 3.b

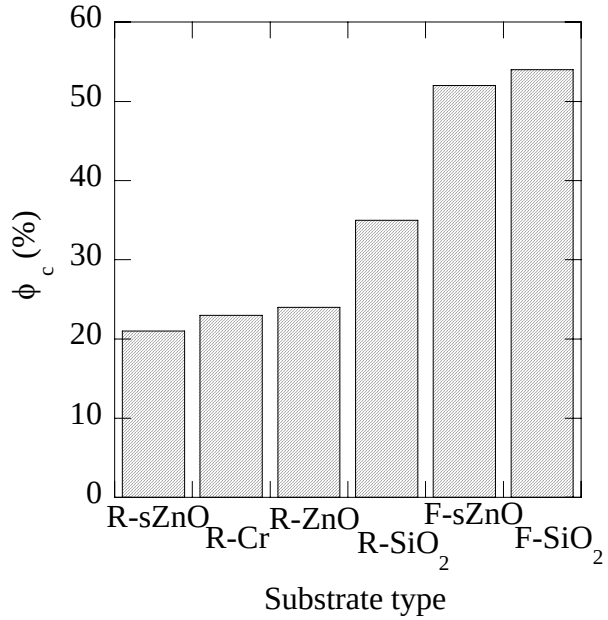
60
50
40
30
20
10
0
ϕ_c (%)
R-sZnO
R-Cr
R-ZnO
R-SiO2
F-sZnO
F-SiO2
Substrate type

Fig. 4

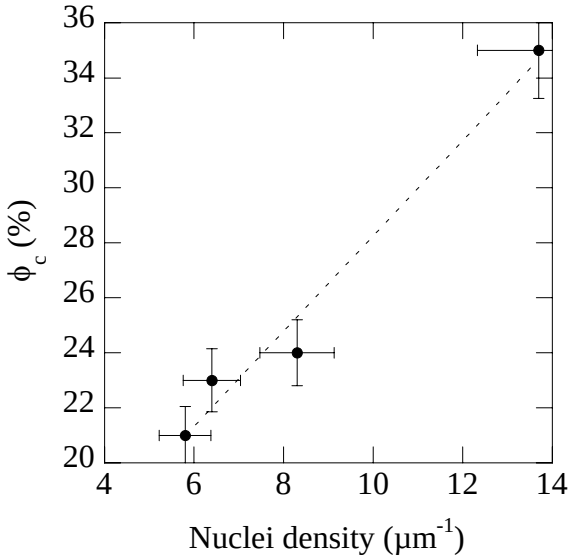
36
34
32
30
28
26
24
22
20
ϕ_c (%)
4
6
8
10
12
14
Nuclei density (μm-1)

Fig. 5